Pair Potential That Reproduces the Shape of Isochrones in Molecular Liquids
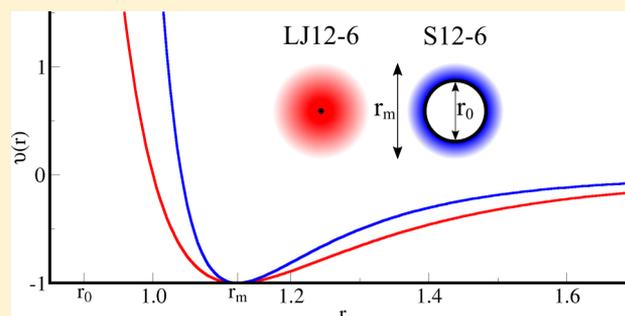
Arno A. Veldhorst,*,[†,‡] Thomas B. Schrøder,[†] and Jeppe C. Dyre[†]

[†]"Glass and Time", IMFUFA, Department of Science and Environment, Roskilde University, P.O. Box 260, DK-4000 Roskilde, Denmark

[‡]Laboratório de Espectroscopia Molecular, Chemistry Institute, University of São Paulo, CP 26077, CEP 05513-970 São Paulo, SP, Brazil

ABSTRACT: Many liquids have curves (isomorphs) in their phase diagrams along which structure, dynamics, and some thermodynamic quantities are invariant in reduced units. A substantial part of their phase diagrams is thus effectively one dimensional. The shapes of these isomorphs are described by a material-dependent function of density, $h(\rho)$, which for real liquids is well approximated by a power law, ρ^γ. However, in simulations, a power law is not adequate when density changes are large; typical models, such as Lennard-Jones liquids, show that $\gamma(\rho) \equiv d \ln h(\rho)/d \ln \rho$ is a decreasing function of density. This article presents results from computer simulations using a new pair potential that diverges at a nonzero distance and can be tuned to give a more realistic shape of $\gamma(\rho)$. Our results indicate that the finite size of molecules is an important factor to take into account when modeling liquids over a large density range.

INTRODUCTION

What controls the dynamics of viscous glass-forming liquids is still an open question.[1−6] Although the dynamics in general depends on both temperature, T, and density, ρ, the dynamics of many organic supercooled liquids can be collapsed onto a single curve when plotted against a combined, material-specific variable, $h(\rho)/T$.[7−9] It was found in many experiments that the scaling function, $h(\rho)$, is generally well approximated by a power law as $h(\rho) = \rho^\gamma$, with γ being the material-specific density-scaling exponent;[10,11] we refer to this as *power-law density scaling*. Another important development was the discovery that the dynamics of liquids is a function of the excess entropy.[12,13]

The isomorph theory[14] explains why both density scaling and excess-entropy scaling work for some liquids. Liquids that obey the isomorph theory have curves in their phase diagram, so-called isomorphs, along which not only the dynamics but also the structure, excess entropy, and other thermodynamic quantities are invariant. The development of the isomorph theory was initiated by the observation that in computer simulations some liquids have strongly correlated fluctuations in their energies and pressures. More specifically, if energy E and pressure p are split into a kinetic part and a configurational part that only depends on particle positions, $\mathbf{R} \equiv (\mathbf{r}_1, ..., \mathbf{r}_N)$, as follows

$$E = K + U(\mathbf{R})$$

$$pV = Nk_B T + W(\mathbf{R}) \tag{1}$$

strong correlations are found between the thermal equilibrium fluctuations of potential energy U and virial W in the NVT ensemble,[15] although strong correlations have also been found at high pressures in the NpT ensemble.[16] Indeed, the standard correlation coefficient

$$R = \frac{\langle \Delta W \Delta U \rangle}{\sqrt{\langle (\Delta W)^2 \rangle \langle (\Delta U)^2 \rangle}} \tag{2}$$

indicates whether a liquid obeys the isomorph theory: this is the case whenever $R > 0.9$ (although this value is of course somewhat arbitrary). The standard linear regression "slope" of the fluctuations

$$\gamma \equiv \frac{\langle \Delta W \Delta U \rangle}{\langle (\Delta U)^2 \rangle} \tag{3}$$

is the density-scaling exponent,[14] and the theory thus provides a convenient way to determine the density-scaling exponent in computer simulations at a single thermodynamic state point.

Another empirical observation that can be explained by the theory is that many liquids have been shown to obey isochronal superposition, meaning that the relaxation spectra of liquids have identical shapes if the average relaxation time is the same.[17−19] Also, several phenomenological melting rules can be explained by the isomorph theory.[20−22] For instance, the

Lindemann melting criterion states that crystals melt when the atomic vibrational displacement reaches a certain value in reduced units. This follows from the theory, as the melting line is predicted to be an isomorph to a good approximation,[14] and indeed, many other properties have also been found to be isomorph invariants along the melting line.[23−25]

Many model systems studied so far have been shown to obey the isomorph theory, including atomic liquids with a range of different pair potentials,[26−29] crystals,[30] as well as rigid[31] and flexible molecular liquids.[32] Experimental evidence for the isomorph theory has proven hard to get but has been provided nonetheless.[33−35] For a detailed description of the isomorph theory, focusing on its validation in simulations and experiments, the reader is referred to a recent Feature article.[36]

The isomorph theory has been tested most thoroughly in computer simulations, making it possible to investigate very large ranges of density. Interestingly, most models that have been simulated show that power-law density scaling does not work, that is, the scaling function $h(\rho)$, which describes the shape of the isomorphs, is *not* a power law.[26−32] Instead, the scaling function $h(\rho)$, which describes the isomorphs via the equation $h(\rho)/T = $ Const., is a more general function of density and depends on the pair potential. Only inverse-power-law (IPL) potentials, with $v(r) \propto r^{-n}$, obey power-law density scaling exactly (with $\gamma = n/3$) and have perfectly correlated fluctuations in U and W ($R = 1$). For other model liquids, $h(\rho)$ is not known analytically, although it can be determined from a single simulation if the pair potential is a sum of IPLs, as is the case for the well-known Lennard-Jones (LJ) pair potential.[37,38] In that case, each power-law term, n, in the potential leads to a term in $h(\rho)$, with the relative contribution of that term to the excess heat capacity, $C_v^{ex} = \sum_n C_{v,n}^{ex}$, as the prefactor[38]

$$h(\rho) = \sum_n \frac{C_{v,n}^{ex}}{C_v^{ex}} \rho^{n/3} \qquad (4)$$

The relative contributions of each term in the potential to C_v^{ex} can easily be determined from a single simulation.

Thus, there is a discrepancy between the simulations that show that power-law density scaling does not work for most model systems and experiments that show that it gives satisfactory collapse for most nonassociating liquids. It is not clear what causes this discrepancy. On the one hand, one could argue that the models used in simulations are too simple to properly capture the physics of real liquids. However, this does not explain why IPL potentials, arguably the simplest pair potentials, *do* predict the power-law density scaling seen in so many different liquids. Indeed, there is no a priori reason why $h(\rho)$ should be a power law; it is used mostly for empirical reasons.

On the other hand, the discrepancy could be explained by the fact that it is much easier to obtain a large range of densities in simulations than it is in experiments. This hypothesis has led to more experimental investigations into liquid dynamics over larger ranges of density.[38−41] Bøhling et al.[38] found that dibutylphthalate (DBP) and decahydroisoquinoline (DHIQ) do not conform to power-law density scaling, although the relaxation time data could still be collapsed when another $h(\rho)$ was used. However, the validity of this analysis is still under discussion, as old and possibly outdated equations of state were used, leading to large extrapolations to determine densities. More recent studies claim to get a good collapse of the data with power-law density scaling for both DHIQ[40] and DBP.[41]

Simulation data and the analysis by Bøhling et al. find an $h(\rho)$ that is not a power law, meaning that the logarithmic slope

$$\gamma(\rho) = \frac{\mathrm{d} \ln h(\rho)}{\mathrm{d} \ln \rho} \qquad (5)$$

which gives the "local" density-scaling exponent, is not constant. Computer simulations of various pair potentials[26−28] and molecular systems[31,32,42] have found $\gamma(\rho)$ to be a decreasing function of density. The fact that the LJ potential has a decreasing $\gamma(\rho)$ can be understood by considering that at high densities particles are close to each other and feel only the repulsive r^{-12} term. For high densities, γ should thus approach $12/3 = 4$. However, at normal densities (around zero pressure), the attractive r^{-6} term plays an important role, and because it is subtracted, it makes the LJ potential steeper than the r^{-12} IPL. Therefore, at low pressure, the LJ potential has a higher scaling exponent than that expected from its r^{-12} term, and one finds here that $\gamma \approx 6$.[26]

Although there is no consensus on whether $h(\rho)$ is always well described by a power law,[38,40,41] none of the experimental data are in agreement with the fact that $\gamma(\rho)$ decreases with density for standard pair potentials, such as the LJ[26] and Buckingham[27] potentials. This led us to investigate other pair potentials for which the density-scaling exponent does not decrease with increasing density.

As the addition of the attractive term makes $\gamma(\rho)$ a decreasing function in the LJ potential, we instead start with a potential that has an increasing $\gamma(\rho)$. We note that such a potential would mean that particles would feel a steeper repulsion as the interparticle distance decreases. This led us to suggest a sum of infinitely many power laws

$$\int_p^\infty r^{-n} \, \mathrm{d}n \qquad (6)$$

as a candidate, as the higher exponents would dominate at shorter r values. For it to be a more realistic model of a molecular liquid, we also include an attraction as

$$A\int_p^\infty r^{-n} \, \mathrm{d}n - B\int_q^\infty r^{-n} \, \mathrm{d}n = A\frac{r^{-p}}{\ln(r)} - B\frac{r^{-q}}{\ln(r)} \qquad (7)$$

with $p > q$. This potential diverges at $r_0 = 1$, but to easily set the potential minimum, r_m, the divergence diameter, r_0, and the potential depth, ε, we parameterize the potential as

$$v(r) = \varepsilon \frac{A(r/r_m)^{-p} - B(r/r_m)^{-q}}{\ln(r/r_0)} \qquad (8)$$

where

$$A = \frac{q \ln(r_m/r_0) + 1}{p - q}$$

$$B = \frac{p \ln(r_m/r_0) + 1}{p - q}$$

In this study, we choose the exponents $p = 12$ and $q = 6$, like those in the standard LJ (LJ12-6) potential, and we designate it as the S12-6 potential due to the integral in eq 6. The potential reduces to the standard LJ potential in the limit $r \to 0$. In the limit $r_0 \to r_m$, the potential becomes purely attractive.

The S12-6 potential aims to reproduce the experimental change in the potential steepness with density, not the steepness of the interatomic interaction itself. Taking the

LJ12-6 as the starting point and "adding" a divergence at r_0, the S12-6 potential is steeper than the LJ12-6 potential, and more so at short distances (see Figure 1). It is known that in many
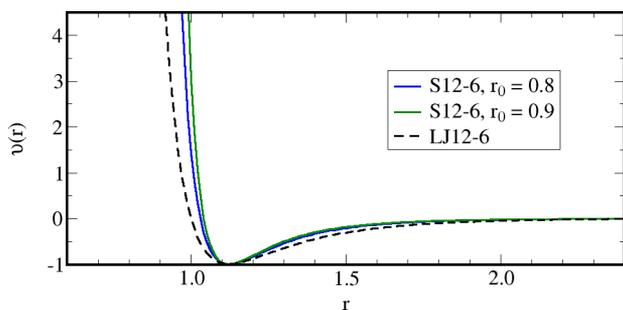

Figure 1. S12-6 pair potential as described in eq 8, plotted for two values of r_0. The minimum was kept at $r_m = 2^{1/6}$ to make the two potentials comparable to the standard LJ12-6 potential, which is shown by the dashed line.

cases the LJ12-6 potential is too steep,[27,43−45] so the same will be true for the S12-6 potential. However, the steepness of the S12-6 potential around the minimum can easily be tuned using exponents p and q.

METHODS

The S12-6 pair potential is plotted in Figure 1. To obtain densities comparable to those of LJ liquids, the position of the potential minimum was chosen to be the same ($\varepsilon = 1$ and $r_m = 2^{1/6}$). This means that we use the LJ parameter $\sigma = 2^{-1/6} r_m$ as the unit of length. Two values of the divergence diameter were simulated ($r_0 = 0.8\sigma$ and 0.9σ). The ratio r_0/r_m can be considered a measure of the steepness of the repulsion; it is 0.713 and 0.802, respectively, in these cases. The potential was cut and shifted at 2.5σ.

A cubic box with periodic boundary conditions and 1000 particles was simulated in the NVT ensemble with a Nosé-Hoover thermostat. The integration time step was 0.001 for most state points, but it was decreased at high temperatures and densities to prevent unphysically large particle displacements. At each state point, an initial configuration was first randomized by simulating 4×10^6 time steps at 4 times the desired temperature, followed by an equilibration run and production run of 1.6×10^7 steps at the desired temperature.

The simulations were performed using the RUMD code.[46] This code is optimized for performing molecular dynamics simulations on a graphics processing unit and designed to make the implementation of new pair potentials straightforward.[47]

RESULTS AND DISCUSSION

Configuration **R** is expressed in reduced (dimensionless) units by scaling with the density as $\rho^{1/3}\mathbf{R}$. Two state points, (ρ_1, T_1) and (ρ_2, T_2), are defined as being isomorphic if configurations $\mathbf{R}_1$ and $\mathbf{R}_2$ of those state points, with the same reduced coordinates

$$\rho_1^{1/3}\mathbf{R}_1 = \rho_2^{1/3}\mathbf{R}_2 \tag{9}$$

also have proportional Boltzmann statistical weights[14]

$$\exp\left(-\frac{U(\mathbf{R}_1)}{k_B T_1}\right) = C_{1,2} \exp\left(-\frac{U(\mathbf{R}_2)}{k_B T_2}\right) \tag{10}$$

In practice, this proportionality should hold to a good approximation for most physically relevant configurations of the two state points with the same constant, $C_{1,2}$ (which only depends on the pair of state points). Recently, a more general definition of the isomorph theory has been discovered,[48] but we use here the "older" definition (eq 10), which arises from the new one via a first-order Taylor expansion and is more convenient for generating isomorphic state points in simulations.

The isomorph definition can be used to obtain a set of isomorphic state points from a simulation at an initial state point by rewriting eq 10 as

$$U(\mathbf{R}_2) = \frac{T_2}{T_1} U(\mathbf{R}_1) + k_B T_2 \ln(C_{1,2}) \tag{11}$$

Carrying out a standard equilibrium NVT simulation at some initial state point 1, one calculates for each configuration first $U(\mathbf{R}_1)$ and subsequently $U(\mathbf{R}_2)$ by scaling to a new density, ρ_2, using eq 9. According to eq 11, the energies of the scaled configurations should be linearly proportional to the energies of the initial configurations, with proportionality constant T_2/T_1. In this way temperature T_2, at which the state point at density ρ_2 is isomorphic to state point 1, is found from the slope in a $U(\mathbf{R}_1)$, $U(\mathbf{R}_2)$ plot.

The intermediate scattering function, $F_S(q, t)$, and the radial distribution function, $g(r)$, along two isomorphs are plotted in Figure 2 in reduced units, defined as $\tilde{t} \equiv t\rho^{1/3}\sqrt{k_B T}$ and $\tilde{r} \equiv$
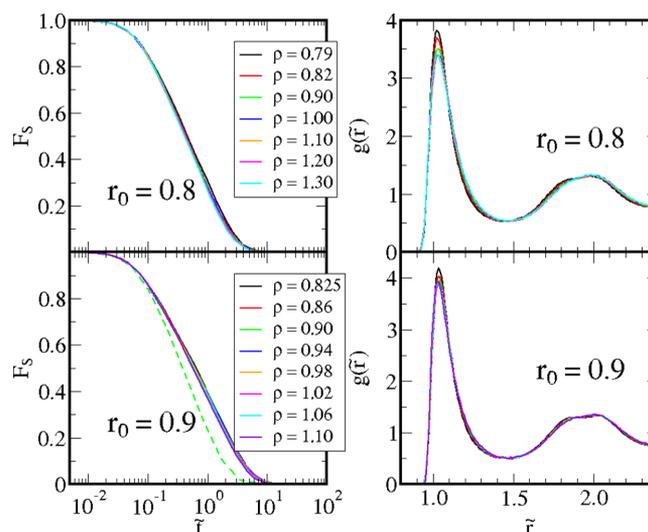

Figure 2. Incoherent intermediate scattering function (left) and radial distribution function (right) in reduced units for the potentials with hard-core diameters $r_0 = 0.8$ (top) and $r_0 = 0.9$ (bottom). For both isomorphs, the dynamics and structure are invariant to a high degree. All intermediate scattering functions have been calculated with the same reduced wave vector ($\tilde{q} = 7.11$). The dashed green line shows the effect of an isochoric ($\rho = 0.9$) temperature change for comparison.

$r\rho^{1/3}$. For $\rho = 0.9$ and $r_0 = 0.9$, the effect on the dynamics of increasing the temperature by a factor of 2 while keeping the density constant is also shown (dashed green line). The isochoric temperature change has a significant effect on the dynamics, whereas there is no significant change in F_S along the isomorph, where temperature changes by a factor of 22. These data indicate that we have indeed obtained two sets of isomorphic state points, as both the dynamics and the structure

are invariant in reduced units to a good approximation along the isomorph. There is a small change in the first peak of $g(r)$, though, which is expected, as at high density the particles are close and feel a steeper part of the potential. This leads to a steeper and therefore higher peak in $g(r)$.[29]

The shapes of the isomorphs in the ρ,T plane are shown in Figure 3 in linear (a) and double-logarithmic (b) scales. There
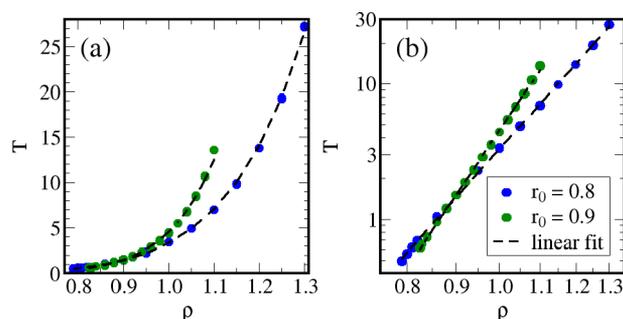

Figure 3. Shapes of the isomorphs in the ρ,T phase diagram on linear (a) and log–log (b) scales. The shapes of the ismorphs are dependent on the hard-core diameter, r_0. On the log–log scale, the isomorphs appear to be fitted well by straight lines (dashed lines).

is a clear effect of particle diameter r_0. For γ to be constant along the isomorph ($h(\rho) \propto \rho^\gamma$), the isomorph should be a straight line in the log–log plot. There is barely any deviation from linear fits (dashed lines) in Figure 3a, indicating that a power law is a good approximation. From the fits, we find approximate "constant γ" values of 7.92 and 10.55, respectively, for $r_0 = 0.8$ and 0.9.

As mentioned, liquids that obey the isomorph theory have strong correlations in the instantaneous values of potential energy U and virial W. We investigate these correlations in Figure 4, plotting correlation coefficient R and "slope" γ from a
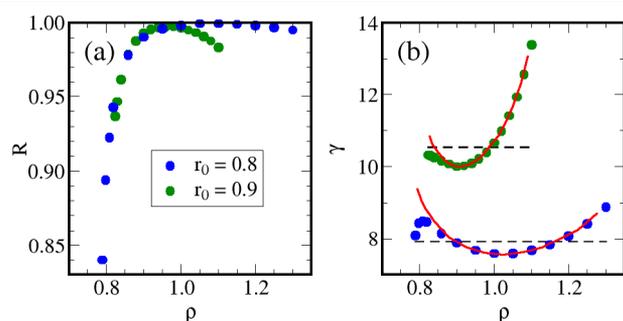

Figure 4. Correlation coefficient R (a) and γ (b) as a function of density, calculated from the fluctuations (eq 2 and eq 3, green and blue dots). The red lines are finite difference estimates (see eq 5) of the data in Figure 3. For both hard-core diameters, r_0, the U, W correlations are strong, and γ increases at high densities.

linear regression of U,W data (eq 3). The liquids have strong correlations at all state points; only close to the gas–liquid coexistence region, at which the pressure becomes negative, is there a significant decrease in R. This is commonly found in many liquids when the pressure approaches zero.[26]

Although the isomorphs are fitted well by a straight line in Figure 3, the change in γ is considerable when calculated from the logarithmic slope of ρ, T data (red line). For both particle sizes, we see an initial decrease in γ with increasing density, similar to what is seen for liquids consisting of point particles,

like LJ liquids.[26] However, unlike such standard systems, γ increases again at higher densities. For $r_0 = 0.8$ the overall variation of the density-scaling exponent is small: $7.5 < \gamma < 8.5$, which is less than that for the LJ potential, considering the large range of densities. Thus, the potential is more in agreement with experimental density-scaling data, although this seems to be caused by the cancellation of a low-density decrease and high-density increase in γ. The density increase is stronger when the hard-core radius is closer to the potential minimum; for $r_0 = 0.9$, γ is clearly not constant, and there is a significant increase at higher densities.

Our results show the importance of potential shape when large density changes are involved, especially when molecular liquids are simulated using coarse-grained models, as in this case it is common to use LJ potentials that diverge at zero distance.[49−51] We note that so far only one other pair potential gives an increasing $\gamma(\rho)$, which is the Girifalco potential.[52,53] This potential was developed to model C_{60} (Buckminsterfullerene), and the size of the C_{60} molecule led to a functional form that also diverges at a nonzero interparticle distance.

CONCLUSIONS

To conclude, our results for the S12-6 pair potential shed light on the discrepancy between experiments and simulations concerning the behavior of the density-scaling exponent, $\gamma(\rho)$. We suggest that the decreasing $\gamma(\rho)$ seen in most simulations is a result of the potential used (often a LJ-type potential). On the other hand, the constant value of γ seen in experiments with molecular liquids seems to be an effect of the finite size of the molecules involved, which is mimicked by the new S12-6 pair potential defined in eq 8. Our results indicate that the size of the molecules should be considered when choosing a pair potential to model a liquid over a large range of densities. Moreover, we predict that for large, bulky molecular liquids, the density-scaling exponent should increase at high densities, as was found in ref 38.

AUTHOR INFORMATION

Corresponding Author
*E-mail: a.a.veldhorst@gmail.com. Phone: +55 11 3091 3853.

Notes
The authors declare no competing financial interest.

REFERENCES

(1) Debenedetti, P. G.; Stillinger, F. H. Supercooled liquids and the glass transition. *Nature* **2001**, *410*, 259−267.
(2) Dyre, J. C. Colloquium: The glass transition and elastic models of glass-forming liquids. *Rev. Mod. Phys.* **2006**, *78*, 953−972.
(3) Lubchenko, V.; Wolynes, P. G. Theory of Structural Glasses and Supercooled Liquids. *Annu. Rev. Phys. Chem.* **2007**, *58*, 235−266.
(4) Kivelson, S. A.; Tarjus, G. In search of a theory of supercooled liquids. *Nat. Mater.* **2008**, *7*, 831−833.
(5) Cavagna, A. Supercooled liquids for pedestrians. *Phys. Rep.* **2009**, *476*, 51−124.
(6) Ediger, M. D.; Harrowell, P. Perspective: Supercooled liquids and glasses. *J. Chem. Phys.* **2012**, *137*, No. 080901.
(7) Tölle, A.; Schober, H.; Wuttke, J.; Randl, O. G.; Fujara, F. Fast relaxation in a fragile liquid under pressure. *Phys. Rev. Lett.* **1998**, *80*, 2374−2377.

(8) Alba-Simionesco, C.; Kivelson, D.; Tarjus, G. Temperature, density, and pressure dependence of relaxation times in supercooled liquids. *J. Chem. Phys.* **2002**, *116*, 5033−5038.

(9) Tarjus, G.; Kivelson, D.; Mossa, S.; Alba-Simionesco, C. Disentangling density and temperature effects in the viscous slowing down of glassforming liquids. *J. Chem. Phys.* **2004**, *120*, 6135−6141.

(10) Roland, C. M.; Hensel-Bielowka, S.; Paluch, M.; Casalini, R. Supercooled dynamics of glass-forming liquids and polymers under hydrostatic pressure. *Rep. Prog. Phys.* **2005**, *68*, 1405−1478.

(11) Roland, C. M. Relaxation phenomena in vitrifying polymers and molecular liquids. *Macromolecules* **2010**, *43*, 7875−7890.

(12) Rosenfeld, Y. Relation between the transport coefficients and the internal entropy of simple systems. *Phys. Rev. A* **1977**, *15*, 2545−2549.

(13) Dzugutov, M. A universal scaling law for atomic diffusion in condensed matter. *Nature* **1996**, *381*, 137−139.

(14) Gnan, N.; Schrøder, T. B.; Pedersen, U. R.; Bailey, N. P.; Dyre, J. C. Pressure-energy correlations in liquids. IV. "Isomorphs" in liquid phase diagrams. *J. Chem. Phys.* **2009**, *131*, No. 234504.

(15) Pedersen, U. R.; Bailey, N. P.; Schrøder, T. B.; Dyre, J. C. Strong pressure-energy correlations in van der Waals liquids. *Phys. Rev. Lett.* **2008**, *100*, No. 015701.

(16) Coslovich, D.; Roland, C. M. Pressure-energy correlations and thermodynamic scaling in viscous Lennard-Jones liquids. *J. Chem. Phys.* **2009**, *130*, No. 014508.

(17) Tölle, A. Neutron scattering studies of the model glass former ortho-terphenyl. *Rep. Prog. Phys.* **2001**, *64*, 1473−1532.

(18) Roland, C. M.; Casalini, R.; Paluch, M. Isochronal temperature-pressure superpositioning of the α-relaxation in type-A glass formers. *Chem. Phys. Lett.* **2003**, *367*, 259−264.

(19) Ngai, K. L.; Casalini, R.; Capaccioli, S.; Paluch, M.; Roland, C. M. Do theories of the glass transition, in which the structural relaxation time does not define the dispersion of the structural relaxation, need revision? *J. Phys. Chem. B* **2005**, *109*, 17356−17360.

(20) Gilvarry, J. J. The Lindemann and Grüneisen Laws. *Phys. Rev.* **1956**, *102*, 308−316.

(21) Ross, M. Generalized Lindemann Melting Law. *Phys. Rev.* **1969**, *184*, 233−242.

(22) Saija, F.; Prestipino, S.; Giaquinta, P. V. Evaluation of phenomenological one-phase criteria for the melting and freezing of softly repulsive particles. *J. Chem. Phys.* **2006**, *124*, No. 244504.

(23) Heyes, D. M.; Dini, D.; Bráka, A. C. Scaling of Lennard-Jones Liquid Elastic Moduli, Viscoelasticity and Other Properties along Fluid-Solid Coexistence. *Phys. Status Solidi B* **2015**, *252*, 1514.

(24) Heyes, D. M.; Bráka, A. C. The Lennard-Jones Melting Line and Isomorphism. *J. Chem. Phys.* **2015**, *143*, No. 234504.

(25) Costigliola, L.; Schrøder, T. B.; Dyre, J. C. Freezing and melting line invariants of the Lennard-Jones system. *Phys. Chem. Chem. Phys.* **2016**, *18*, 14678−14690.

(26) Bailey, N. P.; Pedersen, U. R.; Gnan, N.; Schrøder, T. B.; Dyre, J. C. Pressure-energy correlations in liquids. I. Results from computer simulations. *J. Chem. Phys.* **2008**, *129*, No. 184507.

(27) Veldhorst, A. A.; Bøhling, L.; Dyre, J. C.; Schrøder, T. B. Isomorphs in the Phase Diagram of a Model Liquid without Inverse Power Law Repulsion. *Eur. Phys. J. B* **2012**, *85*, 21.

(28) Bacher, A. K.; Schrøder, T. B.; Dyre, J. C. Explaining why simple liquids are quasi-universal. *Nat. Commun.* **2014**, *5*, No. 5424.

(29) Veldhorst, A. A.; Schrøder, T. B.; Dyre, J. C. Invariants in the Yukawa System's Thermodynamic Phase Diagram. *Phys. Plasmas* **2015**, *22*, No. 073705.

(30) Albrechtsen, D. E.; Olsen, A. E.; Pedersen, U. R.; Schrøder, T. B.; Dyre, J. C. Isomorph invariance of the structure and dynamics of classical crystals. *Phys. Rev. B* **2014**, *90*, No. 094106.

(31) Ingebrigtsen, T. S.; Schrøder, T. B.; Dyre, J. C. Isomorphs in Model Molecular Liquids. *J. Phys. Chem. B* **2012**, *116*, 1018−1034.

(32) Veldhorst, A. A.; Dyre, J. C.; Schrøder, T. B. Scaling of the Dynamics of Flexible Lennard-Jones Chains. *J. Chem. Phys.* **2014**, *141*, No. 054904.

(33) Bailey, N. P.; Pedersen, U. R.; Gnan, N.; Schrøder, T. B.; Dyre, J. C. Pressure-energy correlations in liquids. II. Analysis and consequences. *J. Chem. Phys.* **2008**, *129*, No. 184508.

(34) Gundermann, D.; Pedersen, U. R.; Hecksher, T.; Bailey, N. P.; Jakobsen, B.; Christensen, T.; Olsen, N. B.; Schrøder, T. B.; Fragiadakis, D.; Casalini, R.; et al. Predicting the density-scaling exponent of a glass-forming liquid from Prigogine-Defay ratio measurements. *Nat. Phys.* **2011**, *7*, 816−821.

(35) Xiao, W.; Tofteskov, J.; Christensen, T. V.; Dyre, J. C.; Niss, K. Isomorph theory prediction for the dielectric loss variation along an isochrone. *J. Non-Cryst. Solids* **2015**, *407*, 190−195.

(36) Dyre, J. C. Hidden scale invariance in condensed matter. *J. Phys. Chem. B* **2014**, *118*, 10007−10024.

(37) Ingebrigtsen, T. S.; Bøhling, L.; Schrøder, T. B.; Dyre, J. C. Communication: Thermodynamics of condensed matter with strong pressure-energy correlations. *J. Chem. Phys.* **2012**, *136*, No. 061102.

(38) Bøhling, L.; Ingebrigtsen, T. S.; Grzybowski, A.; Paluch, M.; Dyre, J. C.; Schrøder, T. B. Scaling of viscous dynamics in simple liquids: theory, simulation and experiment. *New J. Phys.* **2012**, *14*, No. 113035.

(39) Abramson, E. H. Viscosity of Fluid Nitrogen to Pressures of 10 GPa. *J. Phys. Chem. B* **2014**, *118*, 11792.

(40) Casalini, R.; Roland, C. M. The anomalous dynamics of decahyroisoquinoline revisited. *J. Chem. Phys.* **2016**, *144*, No. 024502.

(41) Casalini, R.; Bair, S. S.; Roland, C. M. Density Scaling and Decoupling in o-Terphenyl, Salol, and Dibutylphthalate. *arXiv:1606:09182* **2016**.

(42) Schrøder, T. B.; Pedersen, U. R.; Bailey, N. P.; Toxvaerd, S.; Dyre, J. C. Hidden scale invariance in molecular van der Waals liquids: A simulation study. *Phys. Rev. E* **2009**, *80*, No. 041502.

(43) Abrahamson, A. A. Repulsive interaction potentials between rare-gas atoms. Homonuclear two-center systems. *Phys. Rev.* **1963**, *130*, 693−707.

(44) Halgren, T. A. Representation of van der Waals (vdW) interactions in molecular mechanics force fields: potential form, combination rules, and vdW parameters. *J. Am. Chem. Soc.* **1992**, *114*, 7827−7843.

(45) Mattsson, T. R.; Lane, J. M. D.; Cochrane, K. R.; Desjarlais, M. P.; Thompson, A. P.; Pierce, F.; Grest, G. S. First-principles and classical molecular dynamics simulation of shocked polymers. *Phys. Rev. B* **2010**, *81*, No. 054103.

(46) Roskilde University Molecular Dynamics. http://rumd.org.

(47) Bailey, N. P.; Ingebrigtsen, T. S.; Hansen, J. S.; Veldhorst, A. A.; Bøhling, L.; Lemarchand, C. A.; Olsen, A. E.; Bacher, A. K.; Larsen, H.; Dyre, J. C. et al. RUMD: A General Purpose Molecular Dynamics Package Optimized to Utilize GPU Hardware Down to a Few Thousand Particles. *arXiv:1505.05094* **2015**.

(48) Schrøder, T. B.; Dyre, J. C. Simplicity of Condensed Matter at its Core: Generic Definition of a Roskilde-Simple System. *J. Chem. Phys.* **2014**, *141*, No. 204502.

(49) Shinoda, W.; DeVane, R.; Klein, M. L. Multi-property fitting and parameterization of a coarse grained model for aqueous surfactants. *Mol. Simul.* **2007**, *33*, 27−36.

(50) Riniker, S.; Allison, J. R.; van Gunsteren, W. F. On developing coarse-grained models for biomolecular simulation: a review. *Phys. Chem. Chem. Phys.* **2012**, *14*, 12423.

(51) Marrink, S. J.; Tieleman, D. P. Perspective on the Martini model. *Chem. Soc. Rev.* **2013**, *42*, 6801−6822.

(52) Girifalco, L. A. Molecular Properties of C_{60} in the Gas and Solid Phases. *J. Phys. Chem.* **1992**, *96*, 858−861.

(53) Bailey, N. P.; Bøhling, L.; Veldhorst, A. A.; Schrøder, T. B.; Dyre, J. C. Statistical Mechanics of Roskilde Liquids: Configurational Adiabats, Specific Heat Contours, and Density Dependence of the Scaling Exponent. *J. Chem. Phys.* **2013**, *139*, No. 184506.